Rate-Determining Steps in Phenacetin Oxidations by Human Cytochrome P450 1A2 and Selected Mutants†

Chul-Ho Yun, Grover P. Miller, and F. Peter Guengerich*

Department of Biochemistry and Center in Molecular Toxicology, Vanderbilt University School of Medicine, Nashville, Tennessee 37232-0146

Received April 17, 2000; Revised Manuscript Received June 27, 2000

ABSTRACT: Mutants with altered activities were obtained from random libraries of human cytochrome P450 (P450) 1A2 with the putative substrate recognition sequences (SRS) mutated [Parikh, A., Josephy, P. D., and Guengerich, F. P. (1999) *Biochemistry* 38, 5283−5289]. Six mutants from SRS 2 (E225I, E225N, F226I, and F226Y) and 4 (D320A and V322A) regions were expressed as oligohistidine-tagged proteins, purified to homogeneity, and used to analyze kinetics of individual steps in the catalytic cycle, to determine which reaction steps have been altered. When the wild-type, E225I, E225N, F226I, F226Y, D320A, and V322A proteins were reconstituted with NADPH-P450 reductase, rates of 7-ethoxyresorufin *O*-deethylation and phenacetin *O*-deethylation were in accord with those expected from membrane preparations. Within each assay, the values of k_{cat}/K_m varied by 2−3 orders of magnitude, and in the case of E225I and E225N, these parameters were 7−8-fold higher than for the wild-type enzyme. The coupling efficiency obtained from the rates of product formation and NADPH oxidation was low (<20%) in all enzymes. No correlation was found between activities and several individual steps in the catalytic cycle examined, including substrate binding, reduction kinetics, NADPH oxidation, and H_2O_2 formation. Quench reactions did not show a burst for either phenacetin *O*-deethylation or formation of the acetol, a minor product, indicating that rate-determining steps occur prior to product formation. Inter- and intramolecular kinetic deuterium isotope effects for phenacetin *O*-deethylation were 2−3. In the case of phenacetin acetyl hydroxylation (acetol formation), large isotope effects [$^{D}k_{cat}$ or $^{D}(k_{cat}/K_m) > 10$] were observed, providing evidence for rate-limiting C-H bond cleavage. We suggest that the very high isotope effect for acetol formation reflects rate-limiting hydrogen atom abstraction; the lower isotope effect for *O*-deethylation may be a consequence of a 1-electron transfer pathway resulting from the low oxidation potential of the substrate phenacetin. These pre-steady-state, steady-state, and kinetic hydrogen isotope effect studies indicate that the rate-limiting steps are relatively unchanged over an 800-fold range of catalytic activity. We hypothesize that these SRS mutations alter steps leading to the formation of the activated Michaelis complex following the introduction of the first electron.

The microsomal P450s[1] are the major enzymes involved in the oxidation of xenobiotic chemicals in eukaryotes (*5*). Although a few general catalytic mechanisms appear to be operative for most of the reactions catalyzed by the P450s (Scheme 1) (*7*), certain features such as rate-limiting steps and substrate interactions can vary considerably depending on the particular P450 and the reaction involved (*8*). Possible rate-limiting steps in P450 catalysis include substrate binding, reduction, oxygen binding to ferrous P450, addition of the second electron to the system, rearrangement to the final active oxygen species, C-H bond cleavage, product release,

Scheme 1: General Mechanism of P450 Catalysis[a]

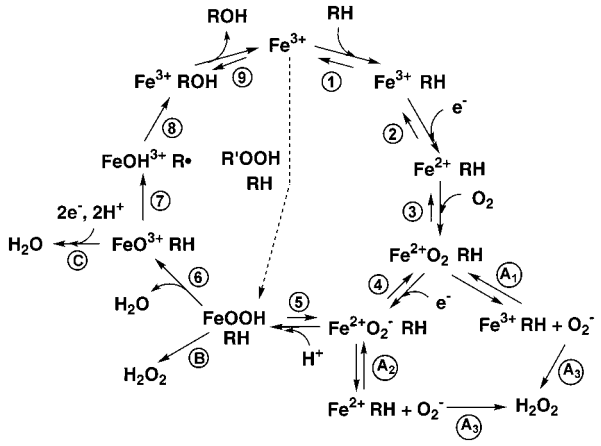

[a] Refs *6* and *7*.

* To whom correspondence should be addressed: Prof. F. Peter Guengerich, Department of Biochemistry and Center in Molecular Toxicology, Vanderbilt University School of Medicine, 638 Medical Research Building I, 23rd and Pierce Avenues, Nashville, TN 37232-0146. Telephone: 615-322-2261. Fax: 615-322-3141. E-mail: guengerich@toxicology.mc.vanderbilt.edu.

† This work was supported in part by United States Public Health Service (USPHS) Grants R35 CA44353 and P30 ES00267. G.P.M. was supported in part by USPHS postdoctoral fellowship F32 GM19808.

[1] Abbreviations: P450, cytochrome P450 [also termed "heme-thiolate P450" by Enzyme Commission (EC 1.14.14.1) (*1*)]; SRS, substrate recognition sequence (*2*); DLPC, L-α-dilauroyl-*sn*-glycero-3-phosphocholine; CHAPS, 3-[(3-choloamidopropyl)-dimethylammonio]-1-propanesulfonic acid; SCE, saturated calomel electrode. The conventions used for the kinetic deuterium isotope effects are those of Northrop (*3*, *4*): $^{D}V = {}^{H}k_{cat}/{}^{D}k_{cat}$ and $^{D}(V/K) = ({}^{H}k_{cat}/{}^{H}K_m)/({}^{D}k_{cat}/{}^{D}K_m)$.

10.1021/bi000869u CCC: $19.00
Published on Web 08/19/2000

and any protein rearrangements (Scheme 1). Little information is available about the rate-limiting step(s) in the human P450 1A2 catalytic cycle.

Human P450 1A2 was first characterized as a phenacetin *O*-deethylase (*9*, *10*); however, this enzyme (located predominantly in the liver) participates in the metabolism of a variety of compounds including the activation of potentially carcinogenic aryl and heterocyclic amines (*10*, *11*). This information and the wide variablity of expression of P450 1A2 suggest that the enzyme may play a role in cancer susceptibility (*12*). To understand the role of enzyme residues in catalysis in the absence of an X-ray crystal structure, the SRS regions (*2*) of P450 1A2 were subjected to random mutagenesis, and selections were made for altered activity, e.g., activation of the heterocyclic amine 2-amino-3,5-dimethylimidazo[4,5-*f*]quinoline (*13*). The single-site mutants from this study displayed a wide range of activities relative to wild-type P450 1A2. The general hypothesis is that individual residues in P450 1A2 control catalytic selectivity by altering kinetics of specific steps in the reaction cycle (Scheme 1).

In the present work, we systematically examined individual reaction steps of P450 1A2 wild-type and single mutant enzymes derived from the random mutagenesis of SRS regions 2 and 4, in particular E225I, E225N, F226Y, F226I, D320A, and V322A. After these mutant enzymes were purified, the steady-state kinetic parameters k_{cat} and K_m were determined for the marker phenacetin *O*-deethylation reaction. Two of the mutants displaying significantly enhanced (E225I) and compromised (D320A) activities were subjected to more thorough steady-state analysis including the use of deuterated phenacetin. To assess any mutational effects on the affinity for phenacetin and the *O*-deethylation product acetaminophen, the respective dissociation constants (K_d) were determined by fluorescence quenching experiments. The rate of the electron-transfer step following substrate binding was also measured, as well as the coupling efficiency of electrons from NADPH. Taken together, the results provide evidence for the existence of two distinct chemical pathways in the oxidation of phenacetin. Individual residues in the SRS regions have major effects on some steps in both reactions but do not alter the rate-limiting steps.

EXPERIMENTAL PROCEDURES

Chemicals. Acetaldehyde, *tert*-butyl hydroperoxide, acetaminophen, and all deuterated reagents used for synthesis were obtained from Aldrich Chemical Co. (Milwaukee, WI). 7-Ethoxyresorufin was obtained from Molecular Probes (Eugene, OR). [*Ring*-^{3}H]phenacetin was a gift of Dr. F. F. Kadlubar (National Center for Toxicology Research, Jefferson, AR). Other chemicals were of the highest grade commercially available.

Synthesis of Substrates and Products. *N*-(4-[1,1-^{2}H]Ethoxyphenyl)acetamide (phenacetin-d_2) was prepared as described (*14*) and recrystallized twice from CH_3OH/H_2O [mp 133−134 °C (uncorr), lit 134−135 °C (*15*)].

N-(4-Ethoxyphenyl)[2,2,2-^{2}H]acetamide (phenacetin-d_3) was synthesized as described (*16*) and recrystallized twice from CH_3OH/H_2O (mp 133−134 °C). Mass spectra yielded the expected molecular ions for the protiated and deuterated products, and the ^{1}H NMR spectra of d_2 and d_3 phenacetins differed from those of unlabeled compounds only by the lack of the corresponding protons, indicating ≥99% expected isotopic abundance for each compound.

N-(4-[1-^{2}H]Ethoxyphenyl)acetamide (phenacetin-d_1) was prepared from acetaminophen (*N*-(4-hydroxyphenyl)acetamide) and [1-^{2}H]ethyl *p*-toluenesulfonate as described (*14*): [1-^{2}H]-CH_3CH_2OH was prepared by NaB^2H_4 reduction of CH_3CHO (*17*) and used to prepare the intermediate [1-^{2}H]-ethyl *p*-toluenesulfonate (*18*). The mass spectrum indicated the expected molecular ion (MH^+ at *m*/*z* 180) for phenacetin-d_1, indicating ∼98% isotopic abundance. In the ^{1}H NMR spectrum, the coupling pattern at δ1.41 (3H, CH_2CH_3) was changed from a triplet (phenacetin-d_0) to a doublet for phenacetin-d_1. The product formed by acetyl hydroxylation of phenacetin, the acetol *N*-(4-ethoxyphenyl)glycoamide, was synthesized as described (*19*, *20*) and recrystallized twice from ethyl acetate (mp 151−152 °C).

Construction of P450 1A2 Expression Plasmids. Primers for PCR reactions were obtained from the Vanderbilt University DNA Core Facility. Expression media for *Escherichia coli* cultures were obtained from Difco (Detroit, MI). Restriction endonucleases and DNA modification enzymes were from New England Biolabs (Beverly, MA) and Promega (Madison, WI). Isopropylthio-β-D-galactoside was purchased from Research Organics (Cleveland, OH). The cDNAs for P450 1A2 wild-type and mutants cloned into the pCW plasmid were from the previous work (*13*). 3′-Terminal ends of the P450 1A2 mutant constructs were modified to include codons for five histidines, followed by a termination codon. The polymerase chain reactions were performed using *Pfu* polymerase essentially as described by the manufacturer (Stratagene, La Jolla, CA), using a Perkin-Elmer 9600 Thermocycler.

Expression and Purification of Recombinant P450 1A2 Wild-Type and Mutants. Each of the recombinant P450 1A2 wild type and mutant enzymes containing a C-terminal $(His)_5$ tag was prepared from the corresponding P450 1A2 (*13*). Expression of P450 1A2 enzymes in *E. coli* DH5α was accomplished essentially as described, and *E. coli* membranes containing recombinant P450 1A2 were prepared (*21*). Membranes were solubilized for 3 h at 4 °C at a final concentration of 2 mg protein mL^{-1} in 100 mM potassium phosphate buffer (pH 7.4) containing 20% glycerol (v/v), 1.0 mM EDTA, 30 μM α-naphthoflavone, 10 mM β-mercaptoethanol, and 1.0% CHAPS (w/v). The solubilized material was then loaded onto a 1 × 4 cm Ni^{2+}-nitrilotriacetate column (Qiagen, Valencia, CA) that had been preequilibrated with 100 mM potassium phosphate buffer (pH 7.4) containing 20% glycerol (v/v), 0.5 M NaCl, 5 mM imidazole, and 0.5% CHAPS (v/v). Contaminating proteins were removed by extensive washing with the equilibration buffer containing 20 mM imidazole. Recombinant P450 1A2 enzymes were eluted from the column with 100 mM potassium phosphate buffer (pH 7.4) containing 20% glycerol (v/v), 300 mM imidazole, 0.5 M NaCl, and 0.5% CHAPS (w/v). Fractions containing P450 were pooled and dialyzed at 4 °C for 24 h against a 200-fold volume of 100 mM potassium phosphate buffer (pH 7.4) containing 20% glycerol (v/v), 1.0 mM EDTA, and 0.10 mM dithiothreitol, followed by two more changes of the same buffer without dithiothreitol. [With human, rat, and rabbit P450 1A2 enzymes, high

ionic strength (100 mM phosphate) should be maintained to prevent precipitation (*21*).]

Sodium dodecyl sulfate−polyacrylamide gel electrophoresis was used to assess final protein purity, and P450 concentrations were determined by Fe^{2+}·CO versus Fe^{2+} difference spectroscopy (*22*). Protein concentrations were determined by quantitative amino acid analysis (24 h hydrolysis, 6 N HCl, 110 °C) in the Vanderbilt Protein Chemistry Facility.

Spectroscopy. UV−visible spectra were recorded using an Amino DW2a/OLIS instrument (On-Line Instrument Systems, Bogart, GA). Wavelength maxima were determined using the peak finder or second-derivative software. The high-spin content of P450 1A2 enzymes was estimated from the second-derivative spectra of the ferric enzymes as described (*23*). ^{1}H NMR spectra were recorded on a Bruker AM 400 spectrometer operating at 400.13 MHz and 27 °C (Bruker, Billerica, MA). Samples were prepared in $CDCl_3$ or dimethyl sulfoxide-d_6 (100.0 at. % D grade, Aldrich). Mass spectrometry was done with a HP 5890A gas chromatograph (Hewlett-Packard Company, Wilmington, DE) and a Finnigan MAT INCOS 50 mass spectrometry (Finnigan Mat, San Jose, CA) unless noted otherwise.

Estimation of Binding Constants by Fluorescence Titration. Because human P450 1A2 is predominantly high-spin (>80%) (*21*) the usual binding spectral titrations could not be used to determine dissociation constants for substrates and products, and we utilized the change of intrinsic fluorescence upon binding to substrate or product. The intrinsic fluorescence of P450 1A2 was determined in a SPEX Fluorolog spectrophotometer (SPEX, Edison, NJ) using a 1.0-cm path length cuvette at 25 °C. Prior to each measurement P450 1A2 was diluted to 1.0 μM in 100 mM potassium phosphate (pH 7.4) containing DLPC (45 μM) in a final volume of 3.0 mL. Emission spectra were corrected using a solution without enzyme. P450 1A2 intrinsic fluorescence was routinely determined by exciting at 295 nm and detecting the fluorescence emission at 340 nm. Additions of ligands from concentrated stock solutions were made in 1.0-μL increments. The maximum volume increase due to sequential addition of the ligand stock solutions was <2% (v/v). All results were corrected for dilution due to ligand addition. At the concentrations of protein or other additions used, no corrections were necessary due to inner filter effects. The change in fluorescence intensity at 340 nm was measured as a function of ligand concentration. Untransformed fluorescence data were plotted as percent change in fluorescence at 340 nm (%ΔF) versus ligand concentration. The titration data were analyzed to yield a dissociation constant (K_d) and the associated SE by nonlinear least-squares fitting (*24*, *25*).

P450 Catalytic Activity Assays. Initial investigations to determine kinetic parameters (K_m and k_{cat}) were done using fluorescence assays for 7-ethoxyresorufin *O*-deethylation and by radio-TLC for phenacetin *O*-deethylation as described (*9*, *26*).

The reaction mixtures consisted of 0.40 μM P450 1A2, 0.80 μM NADPH-P450 reductase [recombinant rat enzyme expressed in *E. coli* (*27*, *28*)], DLPC (45 μM), 100 mM potassium phosphate buffer (pH 7.4), an NADPH-generating system [0.50 mM $NADP^+$, 10 mM glucose 6-phosphate, and 1.0 IU glucose 6-phosphate dehydrogenase mL^{-1} (*29*)], and varying concentrations of substrate (2.0−200 μM phenacetin or 1.0−50 μM 7-ethoxyresorufin) in a total volume of 0.50 mL. Kinetic parameters (K_m and k_{cat}) were determined using nonlinear regression with Graph-Pad Prism software (San Diego, CA).

Phenacetin *O*-dealkylation activity was determined by HPLC as described (*30*), with slight modification, in the kinetic hydrogen isotope effect studies. Incubations with the reaction mixture were generally done for 10 min at 37 °C, terminated with 0.10 mL of 17% $HClO_4$, and centrifuged (10^3g, 10 min); 1.0 mL of a mixture of $CHCl_3$ and 2-propanol (6:4, v/v) was added to the supernatant to extract the products, followed by centrifugation (twice at 10^3g). The organic layers were combined, and solvent was removed under N_2. The products (acetaminophen and the acetol) were analyzed by HPLC using a Beckman Ultrasphere C_{18} column (4.6 × 250 mm, 5 μm) with the mobile phase $H_2O/CH_3OH/CH_3CO_2H$ (65:35:0.1, v/v/v; flow rate 1.0 mL min^{-1}), monitoring A_{254}. In assays with *tert*-butyl hydroperoxide, only the P450 1A2, DLPC, 100 mM potassium phosphate, and substrate were mixed with 5 mM *tert*-butyl hydroperoxide for 60 s at 37 °C.

Anaerobic Reduction Kinetics. Enzyme mixtures and NADPH (600 μM) solutions were prepared separately, as described for steady-state reactions. When indicated, enzyme mixtures contained 200 μM phenacetin. The solutions were made anaerobic by alternate cycles of vacuum and Ar in a closed system (*31*). Reduction kinetics were monitored in a stopped-flow apparatus (Applied Photophysics SX-18MV instrument, Applied Photophysics, Leatherhead, UK) at 37 °C under an anaerobic CO environment using techniques described elsewhere (*8*). Reduction of P450 1A2 to the Fe^{2+}·CO complex was monitored at 446 nm upon mixing of reconstituted enzymes with NADPH. Data were collected using the Applied Photophysics software system and fitted to exponential equations using a Marquardt−Levenberg algorithm for nonlinear regression analysis. Results were repeated with 6−8 individually monitored reactions and averaged using the manufacturer's software.

NADPH Oxidation. P450 1A2 was reconstituted with NADPH-P450 reductase as described for steady-state phenacetin oxidation experiments. Reconstituted enzyme (950 μL) was preincubated for 3 min at 37 °C in the presence or absence of substrate (200 μM). Reactions were initiated with the addition of 50 μL of 4.0 mM NADPH, and the decrease in A_{340} was monitored for 1 min. UV−visible spectra were recorded using a modified Cary14/OLIS spectrophotometer (On-Line Instrument Systems, Bogart, GA). Rates of NADPH oxidation were calculated using $\epsilon_{340} = 6.22$ mM^{-1} cm^{-1} for NADPH.

H_2O_2 Formation. Reaction systems were prepared as described above, except that the reaction volume was 0.40 mL. Reactions were initiated by adding the NADPH-generating system and were terminated by adding 0.80 mL of cold CF_3CO_2H (3%, w/v) after 60 s. H_2O_2 was determined spectrophotometrically by reaction with ferroammonium sulfate and KSCN as described (*32*).

Kinetic Isotope Effect Determination. Deuterium isotope effects were determined by both noncompetitive and competitive methods (*3*, *4*). In the noncompetitive experiments, P450 1A2 was incubated with unlabeled (d_0) phenacetin or labeled (d_2 or d_3) phenacetin using a range of substrate

concentrations (2.0−200 μM), and the products were analyzed by HPLC as described above. K_m and k_{cat} were determined using nonlinear regression as described above.

Two competitive approaches were also used to measure deuterium isotope effects. First, P450 1A2 was incubated with a 1:1 molar mixture of unlabeled (d_0) and phenacetin labeled with deuterium in the ethoxy group (d_2) (final concentration 200 μM), and the acetaldehyde products were extracted and analyzed by combined gas chromatography/positive-ion electron impact mass spectrometry following derivatization with 2,4-dinitrophenylhydrazine (*33*). The hydrazone derivatives were analyzed as described (*34*). Analytes were separated on a 15-m SPB-1 fused silica capillary column (Supelco, Bellefonte, CA) interfaced to a Hewlett-Packard 5890 mass spectrometer (Hewlett-Packard, Wilmington, DE). Conditions were as follows: injection port 230 °C, transfer line 260 °C, initial column temperature 100 °C and increased to 320 °C at a rate of 25 °C min^{-1}. The [^{1}H]acetaldehyde hydrazone was detected by selected ion monitoring at *m*/*z* 224, and the [^{2}H]acetaldehyde hydrazone was monitored at *m*/*z* 225. The ratio of M/M+1 (*m*/*z* 224/225) was used as an estimate of the apparent $^D(V/K)$ for the dealkylation reaction. The second approach was intramoleular and phenacetin-d_1 was used (-OCHDCH$_3$), with the same analysis of the acetaldehyde by mass spectrometry.

In a similar competitive experiment designed to measure intermolecular competition, a 1:1 molar mixture of unlabeled (d_0) and phenacetin labeled with deuterium in the acetyl group (d_3) was used as the substrate (200 μM). The analysis was done by HPLC/electrospray mass spectrometry (Finnegan MAT TSQ7000, Sunnyvale, CA). The separation of the acetol compound by HPLC was done as described above with slight modification. The ratio of M/M+2 (*m*/*z* 228/230) was used as an estimate of the apparent $^D(V/K)$ for acetyl hydroxylation.

Pre-Steady-State Kinetics. Pre-steady-state phenacetin oxidation reactions were done to determine if a step following product formation is rate-limiting. P450 1A2 (400 pmol) was reconstituted as described above and incubated in the presence of 200 μM phenacetin in a total volume of 0.50 mL. Reactions were initiated by mixing with NADPH (final concentration 0.5 mM) for a period of time ranging from 5 to 60 s at 37 °C. The products were analyzed by HPLC as described above.

Iron−Oxygen Intermediate Formation. The P450 1A2 iron−oxygen complex was monitored using an Amino DW2a/OLIS instrument during steady-state oxidation of phenacetin as described (*35*). The reaction mixtures, containing 1.0 μM P450 1A2, NADPH-P450 reductase (0.10−2.0 μM), DLPC (45 μM), 200 μM phenacetin, and 100 mM potassium phosphate buffer (pH 7.4) in a total volume of 1.0 mL, were preincubated for 10 min at 25 °C. NADPH (final concentration 0.10 mM) was then added to initiate the reaction and scans from 350 and 600 nm were obtained.

RESULTS

Properties of Purified P450 1A2 Mutants. The enzymes used for this study were selected from earlier work (*13*) on the basis of altered catalytic activity (Table 1). All enzymes were expressed in *E. coli* and purified. In our initial studies, in which we used ion-exchange and hydroxyapatite chromatography (*21*), we found that some of the mutant enzymes lost heme. We modified all of the proteins to contain a C-terminal $(His)_5$ tag to expedite purification. The use of Ni^{2+}-nitrilotriacetate affinity chromatography not only reduced the time that the enzymes were subjected to chromatography but also allowed us to work without nonionic detergents, which can be P450 1A2 substrates and interfere (*36*). The final specific content ranged from 4 to 17 nmol of P450/mg of protein. Most of the purified P450 1A2 mutants had high heme content except the Phe226 mutant enzymes, suggesting a possible structural determinant. Intrinsic Trp fluorescence and 1-anilinonaphthalene-8-sulfonic acid binding experiments also provided evidence that the Phe226 mutants have more loose conformations than wild-type and other mutated enzymes (results not presented). The mutant enzymes that contained a significant amount of apoprotein (specific content <14 nmol/mg of protein) were not extensively characterized due to the potential complications in catalytic assays, e.g., unproductive competition for the reductase. The $(His)_5$ sequence did not influence the general patterns of binding and activity by the P450 1A2 mutants (results not presented).

Table 1: Specific P450 Content and Spin State of Purified P450 1A2 Mutants

P450 1A2	specific content (nmol of P450/mg of protein)[a]	holoenzyme P450 (%)[b]	% high-spin
wild-type	16.3	92	82
E225I	16.9	95	79
E225N	16.8	95	82
F226I	3.7	21	34
F226Y	6.1	34	31
D320A	15.2	86	38
V322A	14.2	80	83

[a] None of the P450s contained appreciable amounts of cytochrome P420 (>5%). The heme concentration, measured by the pyridine hemochrome assay (*22*), was identical to the P450 concentration (within 5%) in every case. [b] % P450 containing heme. Based on 17.7 nmol/mg of protein (M_r of His-tagged P450 1A2: 56 370).

The high-spin iron fractions of the different enzymes were estimated by second-derivative analysis of the absorption spectra (*23*). Wild-type human P450 1A2 is almost completely high-spin (*21*). The P450 1A2 enzymes may be classified into two groups based on the spin content: wild-type, E225I, E225N, and V322A were ~80% high-spin and F226I, F226Y, and D320A were ~30% high-spin, indicating that mutations in the SRS regions can change the environment of the heme. Three low activity mutant enzymes (F226I, F226Y, and D320A) showed a shift to low-spin, although the spin state is not correlated to the enzyme activity for rat P450 enzymes (*37*) or with these mutants (e.g., V322A has low activity).

Kinetic Parameters of Purified P450 1A2 Mutants. Six SRS region mutants were chosen, purified, and used to measure two P450 1A2 reactions, 7-ethoxyresorufin and phenacetin *O*-deethylation, using a range of substrate concentrations. Two mutants with high activity, three with low activity, and one with similar activity to wild-type were used for this study. The two substrates are quite structually unrelated, although both generate the product acetaldehyde. The mutants displayed 6- and 100-fold variation in k_{cat} for 7-ethoxyresorufin and phenacetin *O*-deethylation, respectively (Table 2). Only the mutants E225I and E225N had

Table 2: Kinetic Parameters for Purified P450 1A2 Mutants

	ethoxyresorufin *O*-deethylation				phenacetin *O*-deethylation[a]			
P450 1A2	k_{cat} (min^{-1})	K_m (μM)	k_{cat}/K_m	relative k_{cat}/K_m	k_{cat} (min^{-1})	K_m (μM)	k_{cat}/K_m	relative k_{cat}/K_m
wild type	0.90 ± 0.11	27 ± 7	0.033 ± 0.009	1	1.8 ± 0.01	13 ± 2	0.14 ± 0.02	1
E225I	0.81± 0.04	14 ± 2	0.060 ± 0.009	1.8	12 ± 1	10 ± 1	1.2 ± 0.2	8.4
E225N	0.94 ± 0.04	7.0 ± 1.0	0.13 ± 0.02	3.9	9.7 ± 0.4	9.0 ± 1.0	1.0 ± 0.1	7.3
F226I	0.28 ± 0.03	22 ± 4	0.13 ± 0.003	0.39	0.18 ± 0.02	15 ± 4	0.012 ± 0.003	0.09
F226Y	0.18 ± 0.06	38 ± 24	0.0047 ± 0.0034	0.15	0.29 ± 0.04	47 ± 15	0.0062 ± 0.0022	0.04
D320A	0.14 ± 0.03	86 ± 33	0.0016 ± 0.0007	0.06	0.12 ± 0.02	70 ± 22	0.0017 ± 0.0006	0.012
V322A	0.73 ± 0.05	16 ± 3	0.046 ± 0.009	1.4	1.6 ± 0.2	42 ± 13	0.037 ± 0.012	0.26

[a] The radio-TLC method was used in these assays. The values estimated for the parameters of the D320A have more inherent error than those presented later (Table 6), in which an HPLC method was used.

Table 3: Binding Affinities of Phenacetin and Acetaminophen for P450 1A2 Mutants

	K_d (μM)[a]	
P450 1A2	phenacetin	acetaminophen
wild-type	17 ± 3	31 ± 2
E225I	22 ± 3	24 ± 2
E225N	16 ± 2	46 ± 7
F226I	18 ± 3	31 ± 2
F226Y	18 ± 2	41 ± 3
D320A	12 ± 1	39 ± 5
V322A	20 ± 2	41 ± 7

[a] K_d values were determined by the change of intrinsic fluorescence intensity of enzymes upon binding of the substrate or product.

Table 4: Reduction Rates of Ferric P450 1A2 Enzymes

	reduction rate (min^{-1})		P450 recovered after experiment (%)	
P450 1A2	−	+ phenacetin	−	+ phenacetin
wild-type	610	450	97	93
E225I	650	620	88	89
E225N	610	995	85	85
F226Y	790	700	76	76
D320A	760	1020	69	82
V322A	610	650	80	78

significantly elevated activities toward phenacetin, emphasizing that the effects of any particular mutation are unique to the enzyme−substrate fit and may diverge with different substrates. The k_{cat}/K_m parameter showed more variation than k_{cat}, being particularly low for the F226 and D320A mutants.

Binding Affinities of P450 1A2 Mutants for Phenacetin and Acetaminophen. Dissociation constants (K_d) were determined using the change in intrinsic fluorescence intensity of enzymes upon binding of the substrate (phenacetin) and product (acetaminophen). The SRS region mutations did not yield apparent changes in the binding affinity for substrate (Table 3), with K_d for all enzymes ranging between 12 and 22 μM. The ferric P450 1A2 D320A mutant was mainly low-spin (Table 1), and the addition of phenacetin produced a typical low- to high-spin conversion (Type I difference spectrum). A titration experiment of this type yielded K_s = 13 ± 1 μM, in agreement with the value of 12 ± 1 μM estimated with the fluorescence method (Table 3). The binding affinity for the product acetaminophen was lower than that of the substrate phenacetin in all mutants except E225I, and no direct correlation between activity and binding affinities to substrate or product was found.

Reduction Kinetics of Human P450 1A2 Enzymes. Wild-type P450 1A2 and all of the mutants were reduced rapidly in monophasic reactions, as shown previously for wild-type enzyme (*8*) (Table 4). The rate was rather invariant with regard to the presence of the substrate phenacetin in most mutants, although two mutants (E225N and D320A) showed a ∼1.5-fold increase of the reduction rate in the presence substrate. The rates of ferric P450 reduction are much higher than steady-state rates of NADPH or phenacetin oxidation (vide infra).

NADPH Oxidation and Coupling of P450 1A2 Reactions. P450 1A2 enzymes oxidize NADPH at relatively high rates in the absence of substrate (Table 5). Mutations in the SRS regions affected NADPH oxidation rates, and the presence of phenacetin increased the rate of NADPH oxidation of some mutant P450 1A2 enzymes. The E225 mutant showed an increase (∼60%) in NADPH oxidation in the presence of substrate, but D320A (with low catalytic activity) also showed this increased NADPH oxidation rate. No correlation was found between rates of NADPH and substrate oxidation.

P450 1A2 enzymes showed low coupling efficiency when product formation and NADPH oxidation were compared. The high activity mutants, E225I and E225N, showed an increase of coupling efficiency by ∼3-fold (to ∼20%) as compared to wild type. Low activity mutants (F226I, F226Y, and D320A) showed only 0.02−0.4% coupling.

H_2O_2 Formation. Mutations in the SRS regions did not affect the rate of H_2O_2 formation in the absence of substrate (Table 5). The presence of the substrate phenacetin did not alter the rate of H_2O_2 formation (except with the D320A mutant, 40% increase).

Identification of an Acetol Product of Phenacetin Oxidation. When phenacetin oxidation assays were done with HPLC instead of the traditional radio-TLC assay (*39*, *40*), a new reaction product was observed. Preliminary mass spectral data suggested that the compound had an M_r of 195, resulting from the addition of 16 amu, which could be an oxygen on either the phenyl ring, the nitrogen, or the ethyl or acetyl methyl. The compound was isolated from large scale incubations done with wild-type P450 1A2 using preparative HPLC and identified as the acetol (Scheme 2) by its mp (151−152 °C), UV spectra (λ_{max} 249 nm), HPLC/MS (MH^+ *m*/*z* 196), ^{1}H NMR (dimethyl sulfoxide-d_6): δ 1.03 (t, 3H, CH_2CH_3), 3.97 (s, 2H, $COCH_2OH$), 4.04 (q, 2H, CH_2CH_3), 5.60 (broad, 1H, OH), 6.85−7.55 (m, 5H, Ar), and comparison to the synthesized standard (*19*, *20*), including co-chromatography on HPLC. *O*-Deethylation (∼85%) is the major oxidation pathway, and acetyl hydroxylation (∼15%) is a minor pathway.

Table 5: NADPH Oxidation and H_2O_2 Product Formation by P450 1A2 Mutants

		mnol of prod min^{-1} (nmol of P450)$^{-1}$				
P450 1A2	phenacetin	NADPH oxidation	acetaminophen formation	acetol formation	H_2O_2 formation	H_2O formation[a]
wild type	+	37 ± 2	1.8 ± 0.1	0.33 ± 0.02	11 ± 1	12 ± 1
	−	34 ± 2			9 ± 1	13 ± 1
E225I	+	76 ± 1	11 ± 1	2.2 ± 0.1	11 ± 1	26 ± 1
	−	46 ± 3			15 ± 1	16 ± 2
E225N	+	56 ± 4	9.2 ± 1.0	1.8 ± 0.2	13 ± 1	16 ± 2
	−	37 ± 4			13 ± 1	12 ± 2
F226I	+	75 ± 6	0.18 ± 0.01	nd[b]	10 ± 1	32 ± 3
	−	62 ± 7			12 ± 1	25 ± 4
F226Y	+	51 ± 4	0.18 ± 0.01	nd	12 ± 1	19 ± 2
	−	51 ± 4			9 ± 1	21 ± 2
D320A	+	67 ± 4	0.010 ± 0.001	0.0010 ± 0.0001	21 ± 1	23 ± 2
	−	42 ± 2			15 ± 1	14 ± 1
V322A	+	45 ± 3	1.2 ± 0.2	nd	10 ± 1	17 ± 2
	−	43 ± 3			9 ± 1	17± 2

[a] H_2O formation was determined by calculating the difference between total NADPH utilized and the sum of H_2O_2 and products produced and then dividing by 2, because four electrons would be required to reduce O_2 to H_2O (*38*). No correction was made for any O_2^-, which was not measured. [b] Not determined.

Scheme 2: Oxidations of Phenacetin Catalyzed by Human P450 1A2[a]

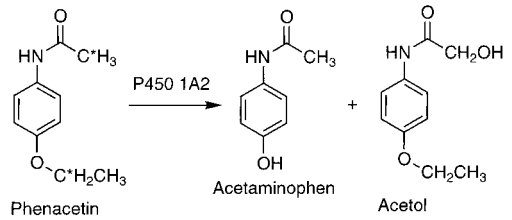

[a] The sites of deuterium substitution utilized in kinetic experiments are labeled with asterisks.

Kinetic Hydrogen Isotope Effects. Wild-type P450 1A2, E225I (high activity), and D320A (low activity) were examined for the rate contribution of C-H bond cleavage to the P450 1A2 catalytic cycle, using deuterium-labeled substrates. Noncompetitive kinetic isotope effects were observed for phenacetin *O*-deethylation [^DV and $^D(V/K)$], 1.9−2.7 in the case of wild-type P450 1A2 and E225I (Table 6). In the case of D320A, the isotope effect was somewhat lower (∼1.5−1.6) as compared to wild-type P450 1A2 and E225I. These results indicate a kinetic contribution of the C-H bond cleavage step in the overall P450 catalytic cycle. In the case of acetyl hydroxylation, a very large intermolecular hydrogen isotope effect [^DV and $^D(V/K) \geq 14$] was observed with all enzymes tested here (Table 6), clearly indicating a rate-limiting contribution of C-H bond cleavage. Substitution of deuterium at each oxidation site did not effect activity at the other site.

To confirm the noncompetitive intermolecular kinetic isotope effect results (e.g., rule out any contribution of substrate impurities), we measured the competitive intermolecular isotope effect, $^D(V/K)$, using wild-type, E225I, and D320A enzymes (Table 7). Both substrates were added together to an incubation mixture (equal concentrations of d_0/d_2 phenacetin for *O*-deethylation or d_0/d_3 phenacetin for acetyl hydroxylation), and a competition between the deuterated and nondeuterated compounds was established, using a single substrate concentration. Competitive kinetic isotope effects [$^D(V/K)$] of 2.7−3.1 were observed for phenacetin O-deethylation in the case of wild-type P450 1A2 and E225I, which are comparable to the noncompetitive intermolecular kinetic isotope effects (Table 6). High isotope effects (≥12) were observed for acetol formation, similar to those obtained in noncompetitive isotope effect experiments.

The intramolecular isotope effects for phenacetin *O*-deethylation were measured in a separate study with phenacetin-d_1 (Table 7). The values were in the range of 1.4−2.2 and, considering the expereimental error, similar to the intermolecular isotope effects.

Phenacetin Oxidation by P450 1A2 Mutants Supported by Peroxides. When *tert*-butyl hydroperoxide was used as an "oxygen surrogate" in place of the reductase, NADPH, and O_2, wild-type P450 1A2 and the E225I mutant showed very low activity (0.2−1.2% of the NADPH-supported reaction) (results not presented). The D320A mutant showed higher activity than the NADPH-supported reaction (k_{cat} = 1.0 min^{-1}).

Iron−Oxygen Intermediate Formation. Wild-type P450 1A2 and the E225I and D320A mutants were compared for their abilities to form a steady-state intermediate species (433 nm, Figure 1). An FeO_2^{2+} intermediate with a similar spectrum has previously been reported for rabbit P450 1A2 (*41*, *42*). The formation of the iron−oxygen intermediate by the D320A mutant was ∼30% that of wild-type P450 1A2 and the E225I mutant. The steady-state level of the complex increased with the concentration of reductase, to reach the indicated level at a reductase/P450 ratio of 2.

Burst Analysis. The time course for product formation was linear for both products, with extrapolation to much less than a single enzyme turnover (Figure 2), indicating that release of products from the active site does not contribute to the overall reaction rates. Therefore, rate-limiting steps must precede product formation.

DISCUSSION

A useful approach to understanding the structure−function relationships underlying catalytic mechanisms of enzymes has been the coupling of random mutagenesis and kinetic characterization of respective mutants. To improve our understanding of P450 1A2 catalysis, we generated single residue mutants of the P450 1A2 SRS regions and screened them on the basis of their ability to activate 2-amino-3,5-

Table 6: Intermolecular Deuterium Isotope Effects on Phenacetin *O*-Dealkylation and Acetyl Hydroxylation by P450 1A2

P450 1A2	phenacetin d_n	*O*-deethylation (acetaminophen formation)					acetyl hydroxylation (acetol formation)				
		k_{cat} (min^{-1})	K_m (μM)	k_{cat}/K_m	^DV	$^D(V/K)$	k_{cat} (min^{-1})	K_m (μM)	k_{cat}/K_m	^DV	$^D(V/K)$
wild type	d_0	1.8 ± 0.1	16 ± 1	0.11 ± 0.01			0.35 ± 0.01	17 ± 2	0.021 ± 0.003		
	d_2	0.93 ± 0.03	18 ± 2	0.052 ± 0.006	1.9 ± 0.1	2.1 ± 0.3	0.37 ± 0.01	18 ± 2	0.021 ± 0.003	0.95 ± 0.04	1.0 ± 0.2
	d_3	1.9 ± 0.1	19 ± 2	0.10 ± 0.01	0.95 ± 0.07	0.91 ± 0.12	0.025 ± 0.003	30 ± 10	$8.3 \times 10^{-4} \pm 2.9 \times 10^{-4}$	14 ± 2	25 ± 9
E225I	d_0	11 ± 1	11 ± 1	1.0 ± 0.01			1.2 ± 0.1	22 ± 3	0.055 ± 0.009		
	d_2	5.5 ± 0.2	15 ± 2	0.37 ± 0.05	2.0 ± 0.02	2.7 ± 0.5	1.5 ± 0.1	26 ± 3	0.058 ± 0.008	0.80 ± 0.09	0.95 ± 0.02
	d_3	11 ± 1	12 ± 2	0.92 ± 0.017	1.0 ± 0.1	1.1 ± 0.2	0.086 ± 0.005	25 ± 4	$3.4 \times 10^{-3} \pm 0.6 \times 10^{-3}$	14 ± 2	16 ± 4
D320A	d_0	0.018 ± 0.001	270 ± 40	$6.7 \times 10^{-5} \pm 1.1 \times 10^{-5}$			$1.4 \times 10^{-3} \pm 0.1 \times 10^{-3}$	25 ± 5	$5.6 \times 10^{-5} \pm 1.2 \times 10^{-5}$		
	d_2	0.011 ± 0.001	250 ± 70	$4.4 \times 10^{-5} \pm 1.3 \times 10^{-5}$	1.6 ± 0.2	1.5 ± 0.5	$1.5 \times 10^{-3} \pm 0.1 \times 10^{-3}$	30 ± 4	$5.0 \times 10^{-5} \pm 0.7 \times 10^{-5}$	0.93 ± 0.09	1.1 ± 0.3
	d_3	0.020 ± 0.002	300 ± 40	$6.7 \times 10^{-5} \pm 1.1 \times 10^{-5}$	0.90 ± 0.10	1.0 ± 0.2	$1.0 \times 10^{-4} \pm 0.1 \times 10^{-4}$	25 ± 5	$4.0 \times 10^{-6} \pm 0.9 \times 10^{-6}$	14 ± 2	14 ± 4

Table 7: Competitive Isotope Effects on Phenacetin *O*-Deethylation and Acetyl Hydroxylation by P450 1A2 Enzymes

	$^D(V/K)$			
	intermolecular[a]		intramolecular[b]	
P450	*O*-deethylation (acetaldehyde formation)	acetyl hydroxylation (acetol formation)	*O*-deethylation (acetaldehyde formation)	
wild-type	2.7 ± 0.2	12 ± 2	1.9 ± 0.1	
E225I	3.1 ± 0.1	12 ± 2	2.2 ± 0.2	
D320A	1.9 ± 0.2	13 ± 3	1.4 ± 0.2	

[a] Equal concentrations (100 μM) of d_0 and d_2 (or d_3) phenacetin were used as substrate. The acetaldehyde (d_0 and d_1) formed by *O*-deethylation activity was analyzed after derivatization with 2,4-dinitrophenylhydrazine. The acetol product was analyzed to measure the relative amounts of d_0 and d_2 products. [b] Phenacetin-d_1 (200 μM) was used as substrate, and analysis was as in footnote *a*. The ratio of *m*/*z* 225/224 (M + 1/M) was used to estimate $^D(V/K)$.

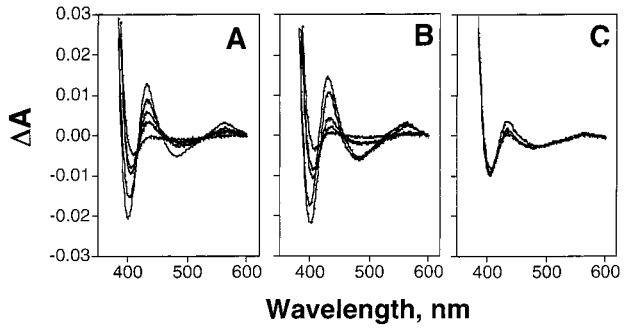

FIGURE 1: Formation of iron−oxygen complex of P450 1A2. The ratio of NADPH-P450 reductase to P450 1A2 was 2. The indicated spectra of (A) wild-type, (B) E225I, or (C) D320A were all recorded 3 min after initiation of reactions.

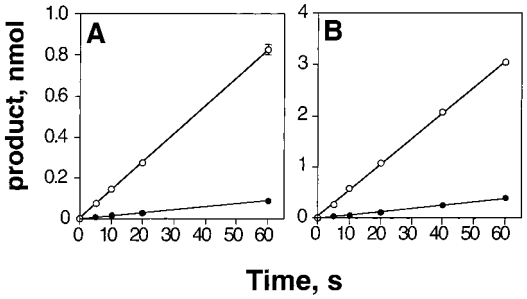

FIGURE 2: Pre-steady-state product formation by P450 1A2. (A) Wild-type and (B) E225I P450 1A2 were used for burst analysis of formation of acetaminophen (○) and the acetol (●).

dimethylimidazo[4,5-*f*]quinoline to a mutagen in a prior study (*13*). Here, several of these P450 1A2 mutants were studied in detail including most of the readily defined steps in the generally postulated catalytic cycle (Scheme 1). A goal of this work was to assess the nature of the effects of the amino acid substitutions on catalytic turnover of phenacetin, a common marker substrate for P450 1A2. These P450 1A2 mutants varied in catalytic efficiency from 0.01 to 8 times the wild-type phenacetin *O*-deethylation activity.

The complex P450 catalytic cycle involves multiple steps that ultimately result in the hydroxylation of the substrate (Scheme 1). In the *O*-deethylation reaction, this product decomposes to yield acetaminophen and acetaldehyde. Further analysis of the products of the P450 1A2-catalyzed reaction revealed that a minor acetol product is also formed (~15% total product). The acetol product had been previ-

ously observed as a minor in vivo product of phenacetin metabolism in rabbits (*19*, *20*). We found no evidence for other potential oxidation products, i.e., either of the two phenols, *N*-hydroxyphenacetin, or the hydroxyethyl product (*19*).

Both of the phenacetin products are formed by C-H bond cleavage, and the similarity of these two reactions was probed using kinetic deuterium isotope studies. A number of kinetic hydrogen isotope studies have been done with P450 enzymes (*43*). The generalization is that large intermolecular isotope effects (>2) are rare, arguing against the existence of C-H bond cleavage as a rate-limiting step. However, high intramolecular deuterium isotope effects are common (e.g., range of 6−10) and constitute a key portion of the evidence for a hydrogen atom abstraction mechanism (*43*−*45*). These intramolecular kinetic deuterium isotope effects are generally considered to approximate the intrinsic kinetic isotope effect for the reaction, if issues of prochirality are not involved. The only large P450 intermolecular kinetic deuterium isotope effects on k_{cat} reported (>2) are for (i) the oxidative *O*-dealkylation of carboxylic acid esters (∼12) (*17*, *46*) and (ii) the *O*-deethylation of 7-ethoxycoumarin by some P450s (5.5) (*47*).[2] It is of interest to note that the latter reaction is a cleavage of an alkyl aryl ether by C-H bond cleavage on the alkyl group, similar to phenacetin O-deethylation.

In this work, we repeatedly found very high kinetic deuterium isotope effects (*12*−*14*) for acetol formation (Tables 6 and 7). These provide clear evidence for rate-limiting C-H bond cleavage in this reaction, with wild-type P450 1A2 and both mutants. This is probably a hydrogen atom abstraction process (Scheme 1), in which the strong oxidant FeO^{3+} cleaves the C-H bond homolytically to produce a radical.

If one oxidation reaction with phenacetin yields a high kinetic deuterium isotope effect, how do we interpret a significant but much lower effect for another reaction with the same substrate? The inter- and intramolecular isotope effects were all ∼2 for *O*-deethylation of phenacetin (Tables 6 and 7). Interestingly, for 7-ethyoxycoumarin *O*-deethylation catalyzed by rat P450 1A1, the intrinsic deuterium isotope effect was reported to be 14, and the intermolecular isotope effect was 1.9 (*47*). One possibility is that two binding orientations of phenacetin induce different enzyme−substrate complexes leading to C-H bond cleavage, with the respective substrate-bound complexes demonstrating different rates of formation. For the *O*-deethylation reaction, steps prior to C-H bond cleavage might mask the intrinsic isotope effect but not in acetol formation. However, this suggestion collapses because the intramolecular isotope effect is also ∼2 (Table 7), an approximation of the intrinsic isotope effect (vide infra).

We propose that the *O*-deethylation of phenacetin proceeds in a chemical mechanism different than acetol formation. Mechanistic possibilities other than hydrogen atom abstraction have been proposed, including nonsynchronous concerted and agostic reactions (*49*, *50*). FeOOH- and FeO_2^{2+}-based P450 mechanisms have been proposed (*51*) but not for *O*-dealkylation or carbon hydroxylation. We propose that

Scheme 3: Hydrogen Atom Abstraction and Electron Transfer Pathways in P450 Oxidation[a]

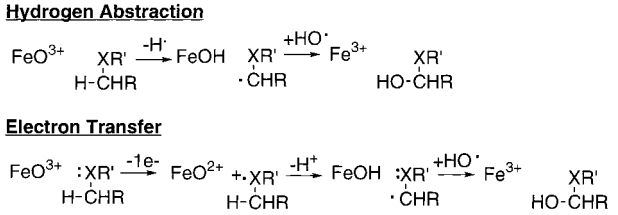

[a] R and R′ are alkyl groups and X denotes a heteroatom (N, O, or S) (*6*, *54*, *57*, *58*).

phenacetin *O*-deethylation involves one-electron oxidation of the substrate. Historically, this mechanism has been invoked for P450 *N*-dealkylations (which often have isotope effects <3) (*52*−*58*), strained cycloalkanes (*59*, *60*), and possibly polycyclic aromatic hydrocarbons (*61*−*64*). A distinction between hydrogen atom abstraction and electron-transfer mechanisms is the propensity for the substrate to undergo one-electron oxidation (Scheme 3). The $E_{1/2}$ for phenacetin is unexpectedly low (0.94 V vs. SCE) (*65*) and falls within the range of a variety of *N*,*N*-dimethylanilines (0.75−1.25 V vs. SCE) (*55*, *56*) and strained alkanes (*66*) believed to undergo the electron transfer mechanism with P450s. Although P450 cleavage of alkyl aryl ethers has not been extensively considered in the context of one-electron transfer, we have recently observed the production of a cation radical of 1,2,4,5-tetramethoxybenzene by rabbit P450 1A2.[3] Charge distribution into the alkoxyl group is expected (*67*), although the issue of kinetic acidity of the alkyl protons has not been considered in regard to P450s (*57*). Subjecting the *O*-deethylation reaction to Hammett or other linear free energy analysis (*54*, *55*, *68*, *69*) will not provide further evidence for one-electron oxidation of phenyl ethyl ethers in that we have found high kinetic deuterium isotope effects for *p*-nitroanisole *O*-demethylation,[4] arguing for a change in the mechanism from one-electron transfer to hydrogen atom abstraction as the $E_{1/2}$ of the substrate increases (*54*).

If the kinetic deuterium isotope effect of ∼2 for phenacetin *O*-deethylation is indicative of a one-electron-transfer mechanism, can it be interpreted in terms of a rate-limiting step? The intramolecular isotope effect is also ∼2 and could be associated with, e.g., rearrangement of the cation radical, but that would be part of the overall reaction.[5] Another likely rate-limiting step in this reaction is the reaction of the iron−oxygen complex, which was found to accumulate (Figure 1). Interestingly, deuteration of the *O*-ethyl methylene did not increase the formation of the minor acetol product. That is, no "switching" (*71*) was observed.

The similar isotope effects among E225I and D320A mutants, as well as wild type, is striking for the formation of the two products. Despite an 800-fold difference in catalytic efficiency, the mechanisms underlying each oxidative reaction do not appear to have been altered. The question then arises as to how can these single mutations result in such dramatic effects on catalysis. Further analyses revealed that the mutational effects were manifested more in catalytic parameters rather than simply binding contacts with substrate phenacetin.

[2] Kinetic deuterium isotope effects of 3−5 on K_m for P450 2E1 reactions have been interpreted in terms of effects on C-H bond cleavage rates in product formation (*34*, *48*).

[3] H. Sato and F. P. Guengerich, *J. Am. Chem. Soc*., in press.

[4] G. P. Miller and F. P. Guengerich, unpublished results.

These mutations did, in fact, alter the organization near the active site as evidenced by shifts in the respective populations of the high- and low-spin state forms of the enzyme (Table 1). Substitution of Phe226 with either Tyr or Ile shifted the predominant heme species from the high-spin (82% for wild type) to the low-spin state (~68% for the mutants), where an H_2O molecule becomes the sixth ligand to the iron. Moreover, the relatively conservative substitutions of Phe226 resulted in a 60−70% loss of bound heme, underscoring its role in heme interaction. In a similar fashion, the removal of Asp320 perturbed the wild-type organization of H_2O molecules in the active site as evidenced by a significant shift to the low-spin state. Substitutions of Glu225 did not change the spin state of the P450. Taken together, analysis of the catalytic parameters for these mutants indicated no correlation with the spin state of the respective mutant.

The alterations of the active site suggested by the shifts in the iron spin-state were also evident from the steady-state studies of phenacetin *O*-deethylation (Table 2). The SRS mutations affected both k_{cat} and K_m values. For Glu225, the removal of a negatively charged residue by substitution with either Ile or Asn greatly enhanced the catalytic efficiency (*8*-fold) of the enzyme for the *O*-deethylation reaction, derived mainly from an increased k_{cat} (Table 2). Moreover, this trend was observed for both oxidative reactions (producing acetaminophen and acetol) with the E225I mutant (Tables 2 and 6). In other words, the mutation enhances a common step(s) during either oxidative pathway for phenacetin. Despite the apparent influence of Phe226 on heme binding, interactions between enzyme and substrate were not perturbed by these mutations (Table 3). Rather, the effects of the mutations were manifest in a decreased rate of substrate dealkylation.The V322A mutant displayed a wild-type turnover rate, but the D320A mutant k_{cat} value was reduced 100-fold as compared to the wild-type rate (Table 6).[6] The F226Y mutant demonstrated an elevated K_m relative to wild type (Table 2). The Ala substitution at Asp320 or Val322 produced mutants whose K_m values increased relative to wild-type P450 1A2. Since the K_d value for phenacetin was not altered by the mutations (Table 3), the respective mutant K_m values must include more than the rate constants describing phenacetin binding. The dissociation constant is probably an apparent K_d value reflecting the contributions of two enzyme−substrate complexes. The observation of two products, acetaminophen and the acetol product, requires two binding orientations for phenacetin. The absence of molecular switching (Table 6) with deuterated substrates argues against rotation within the active site (vide infra), thus the adoption of either binding mode requires phenacetin release and rebinding. The inherent affinity for either binding mode would then be less than the observed K_d value. With regard to phenacetin *O*-deethylation, the higher K_d value for the product acetaminophen (K_d ~30−40 μM) indicates that product inhibition will not likely contribute to steady-state turnover of substrate by these mutants.

Once substrate is bound, there are at least five steps leading up to the carbon−hydrogen bond cleavage step. The rate of reduction of the ferric iron (Scheme 1, step 2) was similar in all cases and much faster than the overall rates of substrate turnover, with or without substrate (Tables 2 and 4). The remaining rates prior to product formation (steps 3−7) are difficult to obtain due to the instability of intermediates (*6*, *69*). To address the impact of the mutations on this portion of the catalytic cycle, the degree of uncoupling was determined for the mutant P450s. In other words, the flow of electrons was followed from NADPH consumption to the production of oxidized product formation, H_2O_2 (step B), and H_2O (step C). Only the H_2O production rates by the E225I and Phe226 mutants were affected by the mutations (~2-fold increase relative to wild type). For these mutants, the FeO^{3+} species is less stable or the substrate is no longer poised for oxidation. For V322A, the H_2O_2 and H_2O formation rates were similar to wild-type values, indicating that decomposition rates of iron−oxygen intermediates within the catalytic cycle had not changed. In contrast, the D320A mutation destabilizes both FeOOH and FeO^{3+} species as measured by the elevated decomposition rates for these intermediates. Taken together, all of the P450s demonstrated relatively poor coupling for phenacetin oxidation with only 20% of the electrons used productively by the best catalyst, the E225N mutant.

Under steady-state conditions, an intermediate formed (λ_{max} 433 nm) in a region of the spectrum where numerous iron−oxygen species have been reported (*35*, *41*, *42*, *72*−*74*). This intermediate is most likely either the $Fe^{2+}O_2$ complex (step 3) or the FeOOH species formed after the protonation of the $Fe^{2+}O_2^{\bullet-}$ species (step 5) based on a variety of studies (*72*, *75*, *76*). The accumulation of this species indicates that either the introduction of the second electron (step 4) or the formation of the FeO^{3+} species (step 6) is slow enough to contribute to steady-state turnover. Without further study it is not possible to distinguish between these scenarios. Of the SRS mutations involved in this study, only D320A

[5] The intramolecular kinetic deuterium isotope effects measured with [*ethyl*-^{2}H]phenacetin (1.4−2.2, Table 7) are not necessarily the intrinsic isotope effects because of the potential issue of prochirality. The interactions of the ^{2}H*R* and ^{2}H*S* atoms (in the racemic substrate) with the protein may differ; the intramolecular experiment would become another competitive intermolecular assay if prochirality is an issue. One approach to the issue is to consider the *O*-methyl homologue of phenacetin as a model, because prochirality is not an issue. We did this experiment with [*O*-methyl-$^2H_2$]methacetin and wild-type P450 1A2, analyzing formaldehyde by mass spectrometry in a manner analogous to the acetaldehyde in Table 7 and estimated an intramolecular isotope effect of 5.4 ± 0.3 (n = 3). This value is greater than the values of 1.9−2.7 measured in the various competitive and noncompetitive phenacetin *O*-deethylation experiments (Tables 6 and 7). However, the value of 5.4 is clearly much less than the isotope effects of ≥14 measured for acetol formation from phenacetin (Table 6). The difference between the intramolecular isotope effects for *O*-deethylation (~2) and *O*-demethylation (5.4) may be due to prochirality and resulting attenuation (vide supra). However, an alternate explanation is that a difference in $E_{1/2}$ of the two substrates may result in a change in the mechanism. The $E_{1/2}$ value for methacetin is reported to be 0.2 V higher than for phencetin (*70*). A lower potential for the ethyl compound may be associated with a shift towards an electron abstraction pathway and lower isotope effect. Nevertheless, the existence of intermolecular isotope effects ≥2 is still of considerable importance, even if they reflect attenuation, in that these values are significantly greater than unity and indicate that C-H bond breaking events are at least partially rate-limiting. The results presented in Figure 2 indicate that the isotope effects cannot be related to any events that occur after product formation, because of the lack of bursts.

[6] For the discussion of the D320A mutant reaction, the steady-state parameters derived from the HPLC technique (Table 6) are used based on the higher sensitivity of this method over the radio-TLC method (Table 2).

demonstrated a 3-fold decrease in the concentration of this intermediate species, which implicates a role in one of these steps in the catalytic cycle; however, the effect of the D320A mutation is not sufficient to account for the large decrease in catalytic efficiency alone.

We conclude that the rate-limiting balance of the individual steps in P450 1A2 catalysis is similar in mutants encompassing an 800-fold difference in catalytic efficiency. Gross substrate affinity appears not to be altered. The formation of the minor product, the acetol, is limited very strongly by C-H bond breaking, as judged by the very high intermolecular kinetic hydrogen isotope effects. For the formation of the major product, acetaminophen, we favor a 1-electron transfer mechanism typically ascribed to *N*-dealkylations to account for the low observed isotope effect for this reaction. The possibility of both oxidative mechanisms contributing to the turnover of a single substrate underscores the plasticity of reaction mechanisms known to be employed by P450s. Taken together, none of the mutational effects on these parameters can account for the variance in catalytic efficiency. In this study, experimental design permitted the assessment of steps leading to the introduction of the first electron (steps 1 and 2 in Scheme 1) and steps following substrate oxidation (steps 7−9). We, therefore, conclude that these SRS mutations alter the intervening steps leading to the formation of the activated Michaelis complex (Scheme 1, steps 3−7), such that the population of enzyme−substrate complexes turning over to product is either increased (E225I and E225N), unaltered (V322A), or decreased (D320A, F226Y, and F226I).

ACKNOWLEDGMENT

We acknowledge the contributions of H. Cai for NMR spectra, I. H. Hanna for helpful discussions, B. Fox and L. Manier for technical assistance with mass spectrometry, and A. Parikh and D. Kim for selection of the P450 1A2 mutants.

REFERENCES

1. Palmer, G., and Reedijk, J. (1992) *J. Biol. Chem. 267*, 665−677.
2. Gotoh, O. (1992) *J. Biol. Chem. 267*, 83−90.
3. Northrop, D. B. (1975) *Biochemistry 14*, 2644−2651.
4. Northrop, D. B. (1982) *Methods Enzymol. 87*, 607−625.
5. Guengerich, F. P. (1995) in *Cytochrome P450: Structure, Mechanism, and Biochemistry, 2nd ed.* (Ortiz de Montellano, P. R., Ed.) pp 473−535, Plenum Press, New York.
6. Ortiz de Montellano, P. R. (1995) in *Cytochrome P450: Structure, Mechanism, and Biochemistry* (Ortiz de Montellano, P. R., Ed.) pp 245−303, Plenum Press, New York.
7. Guengerich, F. P. (1991) *J. Biol. Chem. 266*, 10019−10022.
8. Guengerich, F. P., and Johnson, W. W. (1997) *Biochemistry 36*, 14741−14750.
9. Distlerath, L. M., Reilly, P. E. B., Martin, M. V., Davis, G. G., Wilkinson, G. R., and Guengerich, F. P. (1985) *J. Biol. Chem. 260*, 9057−9067.
10. Butler, M. A., Iwasaki, M., Guengerich, F. P., and Kadlubar, F. F. (1989) *Proc. Natl. Acad. Sci. U.S.A. 86*, 7696−7700.
11. Shimada, T., Iwasaki, M., Martin, M. V., and Guengerich, F. P. (1989) *Cancer Res. 49*, 3218−3228.
12. Turesky, R. J., Constable, A., Richoz, J., Vargu, N., Markovic, J., Martin, M. V., and Guengerich, F. P. (1998) *Chem. Res. Toxicol. 11*, 925−936.
13. Parikh, A., Josephy, P. D., and Guengerich, F. P. (1999) *Biochemistry 38*, 5283−5289.
14. Garland, W. A., Nelson, S. D., and Sasame, H. A. (1976) *Biochem. Biophys. Res. Commun. 72*, 539−545.
15. *Merck Index*, (2000) pp 7344−7345, Merck Research Laboratories, Whitehouse Station, NJ.
16. Fanta, P. E., and Tarbell, D. S. (1955) *Org. Synth. Coll. Vol. 3*, 661−663.
17. Guengerich, F. P., Peterson, L. A., and Böcker, R. H. (1988) *J. Biol. Chem. 263*, 8176−8183.
18. Edgell, W. F., and Parts, L. (1955) *J. Am. Chem. Soc. 77*, 4899−4902.
19. Fischbach, T., and Lenk, W. (1985) *Xenobiotica 15*, 149−164.
20. Kiese, M., and Lenk, W. (1969) *Biochem. Pharmacol. 18*, 1325−1333.
21. Sandhu, P., Guo, Z., Baba, T., Martin, M. V., Tukey, R. H., and Guengerich, F. P. (1994) *Arch. Biochem. Biophys. 309*, 168−177.
22. Omura, T., and Sato, R. (1964) *J. Biol. Chem. 239*, 2370−2378.
23. Guengerich, F. P. (1983) *Biochemistry 22*, 2811−2820.
24. Ehrenberg, M., Cronvall, E., and Rigler, R. (1971) *FEBS Lett. 18*, 199−203.
25. Short, S. A., Armstrong, S. R., Ealick, S. E., and Porter, D. J. T. (1996) *J. Biol. Chem. 271*, 4978−4987.
26. Burke, M. D., and Mayer, R. T. (1983) *Chem.-Biol. Interact. 45*, 243−258.
27. Shen, A. L., Porter, T. D., Wilson, T. E., and Kasper, C. B. (1989) *J. Biol. Chem. 264*, 7584−7589.
28. Hanna, I. H., Teiber, J. F., Kokones, K. L., and Hollenberg, P. F. (1998) *Arch. Biochem. Biophys. 350*, 324−332.
29. Guengerich, F. P. (1994) in *Principles and Methods of Toxicology* (Hayes, A. W., Ed.) pp 1259−1313, Raven Press, New York.
30. von Moltke, L. L., Greenblatt, D. J., Duan, S. X., Schmider, J., Kudchadker, L., Fogelman, S. M., Harmatz, J. S., and Shader, R. I. (1996) *Psychopharmacology 128*, 398−407.
31. Yamazaki, H., Johnson, W. W., Ueng, Y.-F., Shimada, T., and Guengerich, F. P. (1996) *J. Biol. Chem. 271*, 27438−27444.
32. Atkins, W. M., and Sligar, S. G. (1988) *Biochemistry 27*, 1610−1616.
33. Shriner, R. L., Fuson, R. C., and Curtin, D. Y. (1965) in *The Systematic Identification of Organic Compounds*, pp 253−254, Wiley, New York.
34. Bell, L. C., and Guengerich, F. P. (1997) *J. Biol. Chem. 272*, 29643−29651.
35. Guengerich, F. P., Ballou, D. P., and Coon, M. J. (1976) *Biochem. Biophys. Res. Commun. 70*, 951−956.
36. Hosea, N. A., and Guengerich, F. P. (1998) *Arch. Biochem. Biophys. 353*, 365−373.
37. Guengerich, F. P., Dannan, G. A., Wright, S. T., Martin, M. V., and Kaminsky, L. S. (1982) *Biochemistry 21*, 6019−6030.
38. Gorsky, L. D., Koop, D. R., and Coon, M. J. (1984) *J. Biol. Chem. 259*, 6812−6817.
39. Larrey, D., Distlerath, L. M., Dannan, G. A., Wilkinson, G. R., and Guengerich, F. P. (1984) *Biochemistry 23*, 2787−2795.
40. Guengerich, F. P., and Martin, M. V. (1980) *Arch. Biochem. Biophys. 205*, 365−379.
41. Oprian, D. D., Gorsky, L. D., and Coon, M. J. (1983) *J. Biol. Chem. 258*, 8684−8691.
42. Pompon, D., and Coon, M. J. (1984) *J. Biol. Chem. 259*, 15377−15385.
43. Ortiz de Montellano, P. R. (1986) in *Cytochrome P-450* (Ortiz de Montellano, P. R., Ed.) pp 217−271, Plenum Press, New York.
44. Groves, J. T., McClusky, G. A., White, R. E., and Coon, M. J. (1978) *Biochem. Biophys. Res. Commun. 81*, 154−160.
45. Hjelmeland, L. M., Aronow, L., and Trudell, J. R. (1977) *Biochem. Biophys. Res. Commun. 76*, 541−549.
46. Guengerich, F. P. (1987) *J. Biol. Chem. 262*, 8459−8462.
47. Miwa, G. T., Harada, N., and Lu, A. Y. H. (1985) *Arch. Biochem. Biophys. 239*, 155−162.
48. Bell-Parikh, L. C., and Guengerich, F. P. (1999) *J. Biol. Chem. 274*, 23833−23840.
49. Newcomb, M., Le Tadic-Biadatti, M. H., Chestney, D. L., Roberts, E. S., and Hollenberg, P. F. (1995) *J. Am. Chem. Soc. 117*, 12085−12091.

50. Collman, J. P., Chien, A. S., Eberspacher, T. A., and Brauman, J. I. (1998) *J. Am. Chem. Soc. 120*, 425−426.
51. Vaz, A. D. N., Pernecky, S. J., Raner, G. M., and Coon, M. J. (1996) *Proc. Natl. Acad. Sci. U.S.A. 93*, 4644−4648.
52. Abdel-Monem, M. M. (1975) *J. Med. Chem. 18*, 427−430.
53. Miwa, G. T., Zweig, J. S., Walsh, J. S. A., and Lu, A. Y. H. (1980) in *Microsomes, Drug Oxidations, and Chemical Carcinogenesis* (Coon, M. J., Conney, A. H., Estabrook, R. W., Gelboin, H. V., Gillette, J. R., and O'Brien, P. J., Eds.) pp 363−366, Academic Press, New York.
54. Guengerich, F. P., Yun, C.-H., and Macdonald, T. L. (1996) *J. Biol. Chem. 271*, 27321−27329.
55. Macdonald, T. L., Gutheim, W. G., Martin, R. B., and Guengerich, F. P. (1989) *Biochemistry 28*, 2071−2077.
56. Baciocchi, E., Lanzalunga, O., Lapi, A., and Manduchi, L. (1998) *J. Am. Chem. Soc. 120*, 5783−5787.
57. Okazaki, O., and Guengerich, F. P. (1993) *J. Biol. Chem. 268*, 1546−1552.
58. Guengerich, F. P., and Macdonald, T. L. (1993) in *Advances in Electron-Transfer Chemistry, Vol. 3* (Mariano, P. S., Ed.) pp 191−241, JAI Press, Greenwich, CT.
59. Ortiz de Montellano, P. R., Stearns, R. A., and Langry, K. C. (1984) *Mol. Pharmacol. 25*, 310−317.
60. Stearns, R. A., and Ortiz de Montellano, P. R. (1985) *J. Am. Chem. Soc. 107*, 234−240.
61. Fried, J., and Schumm, D. E. (1967) *J. Am. Chem. Soc. 89*, 5508−5509.
62. Ts'o, P. O., Caspary, W. J., and Lorentzen, R. J. (1977) in *Free Radicals in Biology, Vol. III* (Pryor, W. A., Ed.) pp 251−303, Academic Press, New York.
63. Cavalieri, E. L., and Rogan, E. G. (1984) in *Free Radicals in Biology* pp 323−369, Academic Press, New York.
64. Anzenbacher, P., Niwa, T., Tolbert, L. M., Sirimanne, S. S., and Guengerich, F. P. (1996) *Biochemistry 35*, 2512−2520.
65. Miner, D. J., Rice, J. R., Riggin, R. M., and Kissinger, P. T. (1981) *Anal. Chem. 53*, 2258−2263.
66. Stearns, R. A., and Ortiz de Montellano, P. R. (1985) *J. Am. Chem. Soc. 107*, 4081−4082.
67. Baciocchi, E., Bietti, M., Manduchi, L., and Steenken, S. (1999) *J. Am. Chem. Soc. 121*, 6624−6629.
68. Burka, L. T., Guengerich, F. P., Willard, R. J., and Macdonald, T. L. (1985) *J. Am. Chem. Soc. 107*, 2549−2551.
69. Goto, Y., Watanabe, Y., Fukuzumi, S., Jones, J. P., and Dinnocenzo, J. P. (1998) *J. Am. Chem. Soc. 120*, 10762−10763.
70. Hess, U., and Gross, T. (1978) *Z. Chem. 18*, 405−406.
71. Miwa, G. T., and Lu, A. Y. H. (1987) *BioEssays 7*, 215−219.
72. Benson, D. E., Suslick, K. S., and Sligar, S. G. (1997) *Biochemistry 36*, 5104−5107.
73. Ishimura, Y., Ullrich, V., and Peterson, J. A. (1971) *Biochem. Biophys. Res. Commun. 42*, 140−146.
74. Bonfils, C., Debey, P., and Maurel, P. (1979) *Biochem. Biophys. Res. Commun. 88*, 1301−1307.
75. Tajima, K., Edo, T., Ishizu, K., Imaoka, S., Funae, Y., Oka, S., and Sakurai, H. (1993) *Biochem. Biophys. Res. Commun. 191*, 157−164.
76. Shimizu, T., Murakami, Y., and Hatano, M. (1994) *J. Biol. Chem. 269*, 13296−13304.

BI000869U